

A recipe for simulating the observed interhemispheric albedo symmetry and constraining cloud radiative feedbacks

Aiden Jönsson^{1,2}, Maria Rugenstein³, Frida A.-M. Bender^{1,2}, Daniel McCoy⁴,
Trude Eidhammer⁵

¹Department of Meteorology, Stockholm University, 106 91 Stockholm, Sweden

²The Bolin Centre for Climate Research, Stockholm University, 106 91 Stockholm, Sweden

³Department of Atmospheric Science, Colorado State University, 3915 Laporte Avenue, Fort Collins, CO
80521, USA

⁴Department of Atmospheric Science, University of Wyoming, 1000 E. University Avenue, Laramie, WY
82071, USA

⁵National Center for Atmospheric Research, Boulder, CO, USA

Key Points:

- Modeled hemispheric albedo asymmetry in a perturbed parameter ensemble is mostly controlled by extratropical cloud cover
- These simulated cloud asymmetries are primarily caused by precipitation efficiency, cloud phase partitioning, and turbulence
- Shortwave cloud feedbacks constrained with the observed symmetry tend towards stronger positive feedbacks than the model's default settings

Corresponding author: Aiden Jönsson, aiden.jonsson@misu.su.se

Abstract

Earth’s albedo has remained symmetric between the northern and southern hemispheres over the satellite record, a feature that climate models have difficulty capturing. We investigate causes of these biases using a perturbed parameter ensemble of atmospheric simulations to probe the sensitivity of the albedo symmetry to cloud properties and the processes that control them. We find that the most significant parameters to simulated albedo symmetry impact precipitation, turbulent dissipation, and sea salt aerosol emissions. Constraining shortwave cloud feedbacks using the observed albedo symmetry leads to a range of $+0.61 \pm 0.24 \text{ W m}^{-2} \text{ K}^{-1}$ (66% confidence). These are stronger than the model’s control settings due to greater loss of subtropical low clouds and weaker negative cloud phase feedback. Comparing the constrained and control parameter settings shows a preference towards settings that would reduce the control simulation’s biases, indicating that the constraint can select for representations that capture the observed cloud cover.

Plain Language Summary

Despite the northern hemisphere having more reflective land surface area and higher aerosol concentrations than the southern hemisphere, observations show that greater cloud cover and albedo in the southern hemisphere compensates for the clear-sky differences so that the two hemispheres are nearly symmetric in albedo. This feature is not well reproduced by models because of albedo biases, which are in turn caused mostly by parameterized cloud processes. We look at how parameterized processes in an ensemble of simulations in one model impact its hemispheric albedo differences, and investigate the parameter settings that lead to the model reproducing the hemispheric albedo symmetry. The parameter settings that produce a hemispheric albedo symmetry lead to reduced biases relative to the control simulation, and also produce stronger reinforcing climate feedbacks by clouds.

1 Background

Earth’s albedo is remarkably equal in the northern and southern hemispheres (NH and SH, respectively) in both early and modern satellite observations (Vonder Haar & Suomi, 1971; Stevens & Schwartz, 2012; Voigt et al., 2013; Stephens et al., 2015; Datsieris & Stevens, 2021; Jönsson & Bender, 2022). This observation is significant because clouds compensate nearly exactly for the hemispheric asymmetry in clear-sky albedo that results from the higher concentrations of aerosols and land surface area in the NH, despite more ice-covered surface in the SH (Stephens et al., 2015; Diamond et al., 2022; Jönsson & Bender, 2022). While no physical explanation for why hemispheric differences in albedo might be minimized has been found, such an explanation could prove useful in constraining predictions of global cloud cover responses to different forcings, such as anthropogenic greenhouse gas emissions. General circulation models (GCMs) have great difficulty reproducing the albedo symmetry (Stephens et al., 2015; Diamond et al., 2022; Jönsson & Bender, 2022; Rugenstein & Hakuba, 2023; Crueger et al., 2023).

The tropical maximum in cloud cover that follows the rising branch of Hadley circulation has been previously suggested as a compensating mechanism for hemispherically asymmetric heating resulting from clear-sky albedo (Voigt et al., 2014). However, extratropical cloud cover has instead been found to be crucial in compensating for the clear-sky albedo asymmetry (Bender et al., 2017; Datsieris & Stevens, 2021; Jönsson & Bender, 2022). Bender et al. (2017) found that the primary features of cloud cover over ocean that compensate for the clear-sky albedo asymmetry are greater cloud amount in the SH subtropics and both higher cloud amount and albedo in the SH midlatitudes. Datsieris and Stevens (2021) found that cloud cover does not significantly differ over land or ice between the hemispheres, and that higher cloud amount and albedo over ocean – nor-

malized by area – in the SH provides nearly all of the cloud compensations to the clear-sky albedo asymmetry.

Hemispheric differences in the midlatitude storm tracks significantly contribute to the midlatitude cloud albedo asymmetry (Blanco et al., 2023; Hadas et al., 2023), hinting at dynamic processes that may provide the crucial compensating extratropical cloud cover. The weaker NH storminess may be explained with greater surface energy fluxes and stronger circulation due to topographic forcing (Shaw et al., 2022). This links hemispheric differences in surface properties that partly determine the clear-sky albedo asymmetry to atmospheric heat transport and dynamics. Model biases in hemispheric albedo asymmetry are mainly set by SH midlatitude cloud albedo biases, underscoring their importance in compensating for the clear-sky albedo asymmetry (Jönsson & Bender, 2022). SH midlatitude albedo bias has been a long-standing issue in climate models (e.g. Hwang & Frierson, 2013; Bodas-Salcedo et al., 2014) and is attributed to parametric uncertainty (e.g. Vergara-Temprado et al., 2018; Fiddes et al., 2022) and storm track dynamics (Priestley et al., 2023). Sea surface temperatures (SSTs) and surface energy budget biases also play a role in coupled models, creating the possibility for compensating errors (Kay et al., 2016; Hyder et al., 2018; Zhao et al., 2022). These biases may have consequences for simulated climate and climate change projections both locally and globally (Mechoso et al., 2016; Chemke et al., 2022; Kim et al., 2022).

As the relation between model mean-state biases and sensitivities to warming is not well understood (e.g. Dommenges, 2016; Kajtar et al., 2021; Zelinka et al., 2022), it is unclear what role albedo symmetry biases may play in their predictions. Models disagree on their projections of future changes in albedo symmetry in response to anthropogenic aerosol (Diamond et al., 2022) and CO₂ forcings (Rugenstein & Hakuba, 2023; Jönsson & Bender, 2023). Although they agree on a darkening of the NH due to reduced ice cover with warming, models diverge on cloud-driven albedo asymmetry responses, with implications for their shortwave (SW) cloud feedbacks (Jönsson & Bender, 2023).

In this study, we explore how modeled cloud properties and their sensitivities to processes that impact clouds set hemispheric differences in albedo using a perturbed parameter ensemble (PPE) of simulations in one atmospheric model. This allows us to investigate a spread of albedo asymmetries in one model and with direct knowledge of otherwise hard-to-trace parameterizations. Through this, we aim to shed light on discrepancies in simulated albedo symmetry and essential ingredients for reproducing albedo symmetry in climate models.

2 Methods and Materials

We use a PPE of 262 simulations (Eidhammer et al., 2023) made with the Community Atmosphere Model version 6.3 (CAM6), the atmospheric component of the Community Earth System Model version 2 (Danabasoglu et al., 2020), in 1° (nominal) resolution. Each simulation is three years long and uses fixed SSTs and sea ice. We calculate statistics across ensemble members using the time-mean of each member; area averages are calculated using the cosine of latitude as meridional weights (assuming a spherical Earth).

We use simulations made with both present-day (PD) forcings and a warming scenario forcing. PD forcings include fixed sea ice and SSTs (monthly averages for years 1995-2010), and estimates of CO₂ gas concentrations and aerosol emissions averaged over the years 1995-2005. The warming scenario imposes a uniform +4 K warming to the PD SSTs. To estimate SW cloud radiative feedback strengths, we divide the change in global mean SW cloud radiative effect (R_{CRE}) by the change in global mean near-surface air temperature for each PPE member.

Perturbations were made across 45 parameters (see details in Eidhammer et al., 2023) in five CAM6 modules controlling cloud formation and turbulence, cloud microphysics, aerosols and activation, and convection. The parameters contain 13 from the Cloud Layers Unified By Binormals (CLUBB) module (Golaz et al., 2002; Bogenschutz et al., 2013), 13 from the Morrison-Gettelman microphysics module (Gettelman & Morrison, 2015; Gettelman et al., 2015), 7 from the Zhang-McFarlane convection module (Zhang & McFarlane, 1995), 7 from the aerosols and activation (A/A) module, and 4 from the Parameterizations for Unified Microphysics Across Scales module. Perturbations were made simultaneously to all parameters across ranges of plausible values determined by expert judgment. Combinations of parameter settings were selected using Latin hypercube sampling to provide full coverage over the parameter space without introducing spurious correlations.

To investigate the parameter space, we train Gaussian process emulators on the PPE's hemispheric albedo asymmetries and SW cloud radiative feedback strengths using the Earth System Emulator Python module (Watson-Parris et al., 2021); details on the emulations are given in the supplementary information. We generate 10^6 combinations of parameter settings uniformly and randomly sampled across the same range of perturbations as the PPE for each parameter as inputs to the emulators.

Despite fixed sea ice conditions, clear-sky albedo varies in the PPE due to parameters impacting aerosol representations and differences in surface albedo arising from precipitation. However, given the prominent role of clouds in determining albedo and the hypothesis that clouds might regulate the hemispheric albedo symmetry, we focus our investigation on modeled cloud representations. Because of the length and prescribed conditions of the simulations, we are concerned with simulating the symmetry-establishing cloud cover, but not how it interacts with all possible components (e.g., ocean circulation) of a symmetry-maintaining mechanism. The pattern of SST changes with warming is known to be highly relevant to cloud feedbacks (e.g. Rugenstein et al., 2023). How far these relate to feedbacks quantified over certain periods with specific SST patterns is an open question, and the PPE's construction does not allow us to address this nor how they relate to albedo symmetry maintenance.

3 Results

Figure 1a-b shows R_{CRE} and cloud fraction (f) bias in the PD control simulation relative to observational estimates over the period July 2002-June 2021 from Clouds and the Earth's Radiant Energy System, Energy Balanced and Filled (CERES EBAF), Edition 4.1 (NASA/LARC/SD/ASDC, 2019). The spread in albedo asymmetries (*asymmetry* hereafter defined as NH minus SH hemispheric mean reflected SW radiation) across the PPE's simulations are presented in Figure 1c. These range from ca -18 to +12 W m^{-2} with PD forcings (Figure 1c), a spread much larger than that seen in multi-model ensembles (Stephens et al., 2015; Jönsson & Bender, 2022; Rugenstein & Hakuba, 2023; Jönsson & Bender, 2023). The degree and variability of symmetry seen in CERES EBAF occupies a small portion of this spread.

Despite the large range of asymmetries across the PPE, the PD control simulation exhibits a small degree of asymmetry (-0.13 W m^{-2}) compared to other GCMs ($\sim \pm 5 \text{ W m}^{-2}$). However, Figure 1a-b illustrates that this is the result of compensating regional biases. Clouds in the control simulation reflect too much solar radiation in the tropics and too little in the subtropics relative to CERES EBAF, the latter primarily stemming from too little cloud amount in subtropical eastern ocean basins. The large spread of SW cloud radiative feedbacks in the PPE (Figure 1d) allows us to investigate what cloud properties drive these feedbacks under global warming. In the following, we investigate which properties of the global cloud cover drive the PPE's albedo asymmetry biases (Section

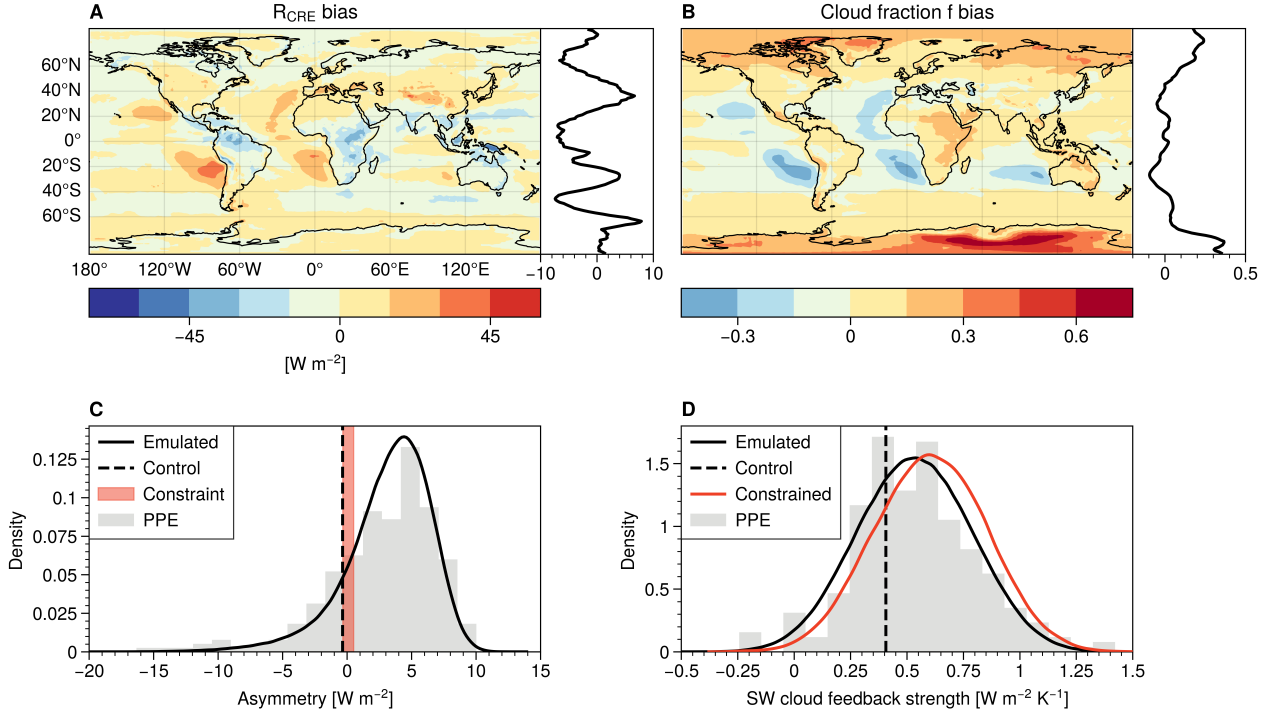


Figure 1. PD control simulation bias in R_{CRE} (a) and cloud fraction (b), relative to the 20-year mean of CERES EBAF (meridional profiles of zonal mean bias in W m^{-2} are included at the right of each map), and probability density distributions of albedo asymmetry (c) and SW cloud radiative feedback strengths (d). Grey bars are 20-bin histograms and curves are kernel density estimates of emulations fitted to the distributions. Solid vertical lines represent CAM6 control simulation asymmetry and SW cloud feedbacks. The red vertical shading in (c) represents the constraint range of asymmetry seen in CERES EBAF (a standard deviation of 12-month running means from the 20-year mean), and the red curve in (d) are the constrained emulated SW cloud feedbacks (see Section 3.3).

3.1) and which parameters contribute most to them (Section 3.2); we will return to SW cloud feedbacks in Section 3.3.

3.1 Ingredients for Hemispherically Asymmetric Cloud Cover

Model parameterizations communicate variables from resolved large-scale processes to unresolved small-scale processes that in turn impact the climate system. Cloud parameterizations translate large-scale dynamic and thermodynamic processes to their effects on cloud formation and properties, which in turn determine their radiative effects. To estimate the degree of influence that each cloud property has on the albedo asymmetry across the PPE simulations, we calculate mutual information (MI; Cover & Thomas, 2005) between simulated albedo asymmetry and hemispheric asymmetries in five cloud properties: in-cloud liquid and ice water paths (LWP and IWP, respectively), cloud amount f , liquid droplet number concentration N_D , and cloud ice fraction f_I , given as the ratio of IWP to the total cloud water content (LWP + IWP). MI is a measure of how much uncertainty in predicting one variable is reduced by knowledge of another; the details of these calculations can be found in the supplementary information. We find that the cloud properties of significant (with $p < 0.05$) importance to simulated albedo asym-

metry are, in descending order: LWP, cloud fraction, droplet concentration, and cloud ice fraction. Figure 2 displays maps of geographic covariances between simulated albedo asymmetry and these properties across the PPE, calculated independently for each grid cell along the ensemble member dimension.

In the tropical western Pacific, higher cloud fraction is associated with more positive albedo asymmetry (Figure 2b), likely by reinforcing the tropical cloud asymmetry driven by the northerly mean position of the ITCZ (Bender et al., 2017). Extratropical clouds play a more prominent role in the simulated albedo asymmetry. LWP covaries most heavily with albedo asymmetry in the midlatitudes, with increased LWP associated with negative asymmetries (Figure 2a). Subtropical and midlatitude cloud fraction covary with albedo asymmetry, with reduced f being associated with positive asymmetries (Figure 2a). N_D impacts albedo asymmetry most strongly in the midlatitudes, and higher N_D is associated with more negative asymmetry (Figure 2c). The overall dependence of albedo asymmetry on cloud phase is fairly evenly distributed so that increasing the ice content of clouds increases asymmetry (NH-brighter), but particularly so over subtropical eastern ocean basins and midlatitudes (Figure 2d).

Figure 2 also compares the relation between simulated albedo asymmetries and hemispheric differences in LWP, f , and f_I in 21 Atmospheric Model Intercomparison Project (AMIP) models from the Climate Model Intercomparison Project, phase 6 (Eyring et al., 2016), and in the PPE. These simulations are made using estimates of time varying historical forcings, SSTs, and sea ice concentrations. We compute averages over the years 2000-2014 and across 3 realizations of each model; the list of models, their references, and output used are given in the supplementary information. Across AMIP models, modeled hemispheric differences in cloud fraction have the strongest correlation with albedo asymmetries, followed by LWP. This disagreement points to climate models' multi-generational problem of radiation biases stemming from cloud occurrence biases (e.g. Nam et al., 2012; Bender et al., 2017). That the PPE agrees with AMIP models on the relation between cloud properties and albedo asymmetry increases our confidence that the PPE is meaningfully sampling the sensitivity of modeled albedo symmetry to cloud properties.

To summarize, we find that subtropical cloud amount as well as midlatitude cloud albedo and amount are the most relevant features of global cloud cover to simulated albedo asymmetries across the PPE. That extratropical clouds are the primary driver of albedo asymmetry in the PPE reflects previous findings (Jönsson & Bender, 2022) and their capacity for driving changes in albedo asymmetry (Datseris & Stevens, 2021; Hadas et al., 2023; Jönsson & Bender, 2023). Considering these relations between cloud properties and asymmetry, we ask: what parameterized processes drive these variations in cloud cover across the PPE? In the next section, we present parameters that strongly impact albedo asymmetry in the PPE, and describe how they affect cloud properties and albedo.

3.2 A Recipe for Albedo Symmetry: Sensitivity to Parameters

To estimate the importance of each parameter to simulated albedo asymmetry, we calculate the MI between each parameter's values and albedo asymmetries in PD simulations. In this section, we present the parameters where knowledge of their settings significantly (with $p < 0.05$) reduce uncertainty in predicting asymmetries across the PPE, grouped according to the physical processes that they impact. Details and results of the MI calculations for all parameters are found in the supplementary information. Ten parameters are significant at this confidence level. We divide these parameters into three groups of processes: precipitation, turbulence, and sea salt aerosol emissions (Figure 3).

Of the 10 parameters that impact albedo and cloud asymmetries the most, five impact rain formation rates in liquid clouds, represented in models as the autoconversion, or the transformation of liquid cloud droplets into rain. Two of these belong to the au-

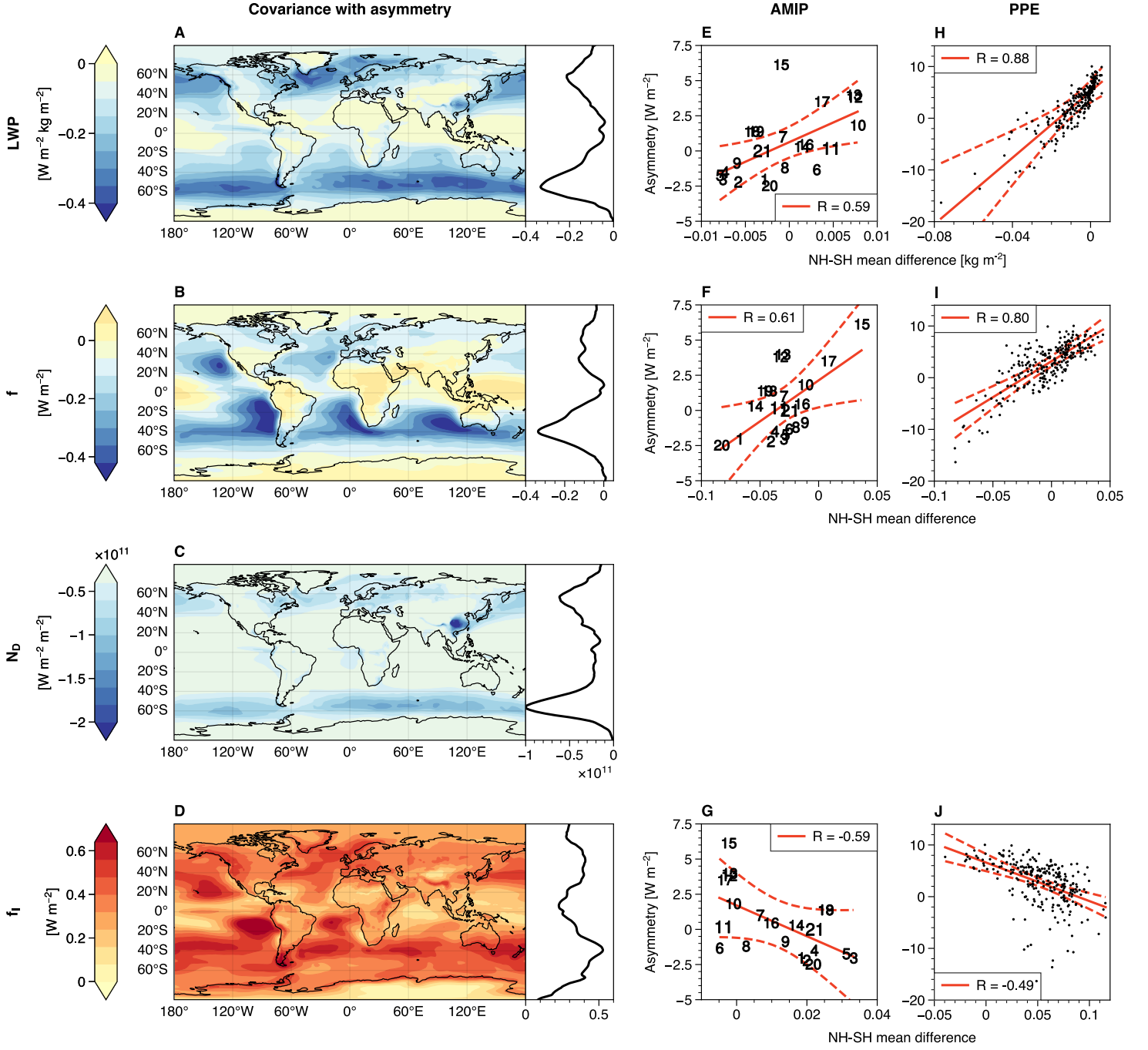


Figure 2. Maps of geographical covariance between the variable and asymmetry: (a) in-cloud liquid water path (LWP), (b) cloud fraction (f), (c) cloud droplet number concentration (N_D), and (d) cloud ice content fraction (f_I). Profiles of zonal means are included to the right of each map, in the same units. Middle column: simulated asymmetries in AMIP models (e-g) and PPE members (h-j) plotted against NH-SH hemispheric mean differences in LWP, f , and f_I . Model numbers (markers) are as listed in Table S1; lines in e-j are ordinary least squares regressions, and dashed lines indicate the fit's 95% confidence interval.

Precipitation

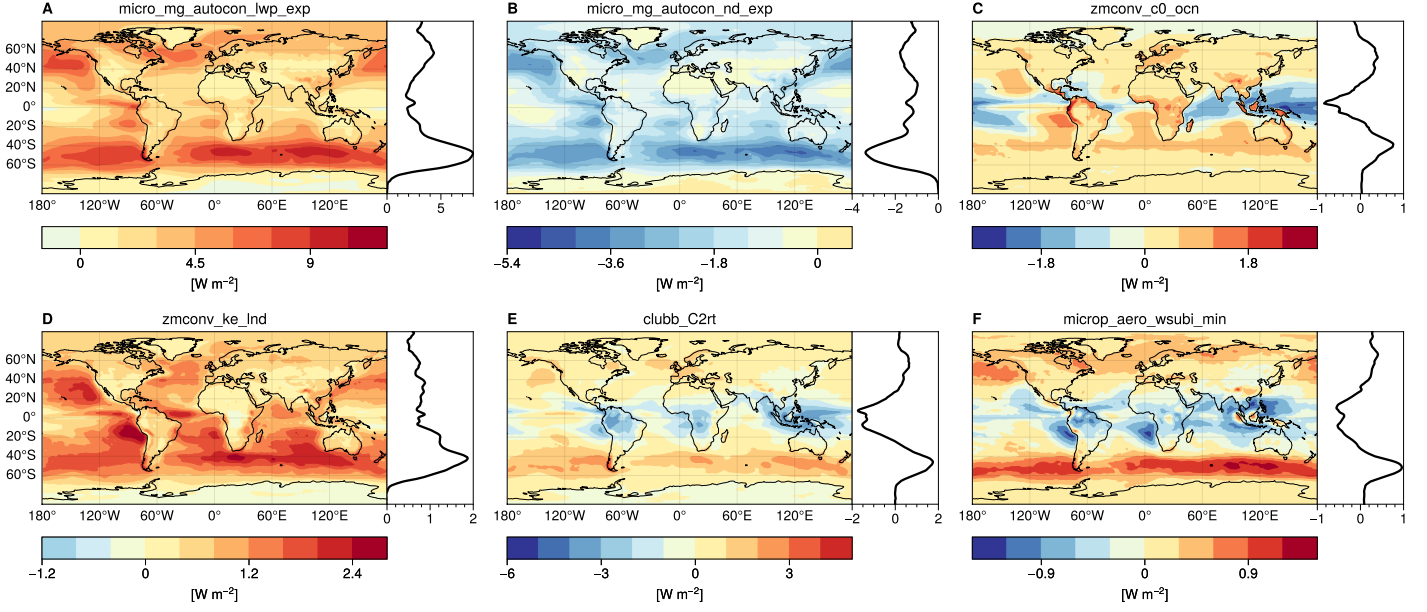


Figure 3. Maps of covariance between parameters' normalized settings and reflected SW radiation across the PPE's PD simulations for parameters that significantly impact the albedo asymmetry in the PPE, grouped according to the processes that they impact: (a-f) precipitation processes, (g-h) turbulence, and (i) sea salt aerosol emissions. To the right of each map is a meridional profile of zonal mean covariance. `clubb_C6th1b` is not shown (see Supplementary Figure S5).

toconversion rate parameterization (from Khairoutdinov & Kogan, 2000; hereafter KK00) implemented in the CAM6 cloud microphysics module. This parameterization is formulated so that autoconversion is exponentially dependent upon LWP and inversely exponentially dependent upon N_D ; the exponents are set with these two parameters. For a given LWP, increasing N_D reduces drizzle formation and extends cloud lifetime. Weakening the dependence upon LWP (N_D) by increasing `micro_mg.autocon_lwp_exp` (decreasing `micro_mg.autocon_nd_exp`) decreases autoconversion, increasing cloud lifetime. Their ability to impact albedo asymmetry stems from higher autoconversion rates decreasing LWP symmetrically over ocean (Supplementary Figure S7) in the NH and SH, but decreasing f more in the SH than in the NH (Supplementary Figure S9).

One parameter from the deep convection scheme (Zhang & McFarlane, 1995; hereafter ZM95), `zmconv_c0_ocn`, impacts autoconversion rates over ocean. In ZM95, convective autoconversion is the product of the coefficient `zmconv_c0_ocn`, upward mass flux, and cloud water content. To similar magnitudes in both hemispheres, increasing `zmconv_c0_ocn` decreases albedo (Supplementary Figures S8 and S10 illustrate that this is via lower LWP and f , respectively) in the tropical western oceans, but increases it in the subtropical eastern oceans and midlatitudes (via higher f , see Supplementary Figure S10). This is likely because it increases cloud sinks in deep convective regimes over tropical western oceans, but impacts trade wind cumulus regions differently in boundary layer interactions (Zhang & McFarlane, 1995). Figure 3c suggests that its hemispherically asymmetric impact stems mostly from the SH’s extensive ocean coverage.

The parameter `clubb_C2rt` dissipates variances in total water mixing ratios and liquid water potential temperatures, smoothing precipitation; increasing this parameter decreases (increases) albedo wherever precipitation is less (more) important to cloud lifetime and thus albedo (Guo et al., 2015). This affects albedo asymmetry by decreasing tropical and subtropical albedo via reduced f , and increasing midlatitude albedo via greater LWP and f . Guo et al. (2015) found that `clubb_C2rt` has an effective control on global low cloud cover (LCC) by strengthening or weakening inversions, and that its impact on LCC is greatest in the midlatitudes where it interacts with autoconversion parameterizations. At high values, `clubb_C2rt`’s interactions with KK00 and other accretion parameters within the microphysics scheme suppress autoconversion by decreasing variances of cloud water content, which is used to determine accretion process rates.

The parameter `microp_aero_wsubi_min` sets minimum subgrid vertical velocities required for freezing activation of aerosols, and links cloud phase partitioning to simulated albedo asymmetry. Increasing this reduces IWP and f_I , and increases LWP and f . This parameter especially impacts SH midlatitude cloud albedo. SH midlatitude clouds are made brighter than their NH counterparts by larger portions of supercooled liquid water, and long-standing biases in modeled phase partitioning have been shown to impact their representations and responses in GCMs (Bodas-Salcedo et al., 2016). This result supports previous findings that asymmetries in midlatitude cloud microphysical properties are important to the hemispheric albedo symmetry (Bender et al., 2017; Datseris & Stevens, 2021; Jönsson & Bender, 2022).

Turbulent boundary layer processes are also important to simulated albedo asymmetry in the PPE. One parameter from the CLUBB scheme, `clubb_C14`, affects simulated albedo asymmetries through damping horizontal wind variances. Increasing the dissipation of horizontal turbulence decreases f and LWP over the subtropics and midlatitudes, but its impact is asymmetrically stronger in the SH midlatitudes. Dissipating horizontal wind variances leads to reduced vertical velocity variances because of continuity, driving a net loss in turbulent kinetic energy. Turbulence-driven moisture transfer between the surface and cloud layer is key to the growth of boundary layer clouds (Wood, 2012). This parameter has also been used in tuning by acting as a dial for global LCC and thus albedo (Golaz et al., 2019, 2022). Two further CLUBB parameters – `clubb_C6rtb` and `clubb_C6th1b` – impact vertical scalar water fluxes within clouds with buoyancy damping, specifically for clouds with highly skewed variances of vertical velocities (i.e. cumuli-form clouds). Because these parameters operate similarly, they are perturbed simultaneously and equally in the PPE. Increasing damping reduces vertical water fluxes, reducing cloud growth in the tropics and subtropics. This lowers albedo by reducing f and LWP.

Finally, the parameter that scales sea salt aerosol emissions (`seasalt_emis_scale`) is significant to simulated albedo asymmetry in the PPE; this parameter increases albedo primarily in the midlatitudes, where surface winds are strongest. The effect of emitting more sea salt aerosols is twofold: first, higher concentrations increase the clear-sky reflectivity of the atmosphere, and second, they act as cloud condensation nuclei for liq-

uid cloud droplets. The latter effect of increased sea salt aerosols is higher cloud albedo through higher N_D and longer lifetime (Fan et al., 2016; Szopa et al., 2021). Figure 3g illustrates that the parameter’s effects are greatest in the SH midlatitudes. The considerable uncertainties of sea salt aerosol emissions, concentrations, and compositions as well as their effects on clouds in both observations and model parameterizations would make them a critical point in representations of albedo symmetry, but the complex connection between aerosols and albedo makes a realistic representation difficult to achieve (de Leeuw et al., 2011; Tsigaridis et al., 2013; Carslaw et al., 2013; McCoy et al., 2015; Hartery et al., 2020).

3.3 Albedo Symmetry as a Constraint

In model development, poorly constrained parameters are often changed in order to tune towards radiative balance closure and reasonable global mean values (Bender, 2008; Mauritsen et al., 2012; Hourdin et al., 2017). Tuning a model presents challenges that require making compromises between variables of interest, hence compensating errors in models that allow them to reasonably capture bulk properties of Earth’s climate system. Using the PPE’s coverage of settings in its parameter space to find combinations of parameters that lead to albedo symmetry allows us to see how tuning a model to the observed albedo symmetry might affect the model’s radiative feedbacks and sensitivity to forcings. Because it is postulated that a mechanism that would maintain hemispheric albedo symmetry would primarily implicate clouds, it would first and foremost affect SW cloud feedbacks. Here we make use of the PPE’s spread in SW cloud feedback strengths to investigate how constraining the parameter space with the observed hemispheric albedo symmetry impacts SW cloud feedbacks. We hypothesize that the model’s climate and feedbacks would behave differently from the control when constrained with the hemispheric albedo symmetry because it could reduce compensating errors by introducing a check based on bulk spatial features of the planetary albedo.

To test this hypothesis, we constrain combinations of parameter settings that lead to emulated albedo asymmetries that fall near the observed degree of albedo symmetry. For the constraint bounds, we use CERES EBAF time-mean hemispheric albedo asymmetry and the standard deviation in 12-month running means over the July 2002–June 2021 period as the constraint bounds. Figure 1c–d shows the emulated distributions of albedo asymmetries and SW cloud feedbacks, the constraint span (Figure 1c), and the distribution of constrained SW cloud feedbacks (dashed curve in Figure 1d). Only 4.8% of the emulated asymmetries lie within the constraint bounds. Constrained parameter setting combinations (Supplementary Figure S4) include a large number of combinations that lead to compensating biases that can yield albedo symmetry; however, their distributions allow us to find where in the parameter range they tend towards when the model produces albedo symmetry.

The albedo symmetry constraint leads to stronger positive SW cloud feedback strengths ($+0.61 \pm 0.24 \text{ W m}^{-2} \text{ K}^{-1}$ for 66% confidence interval bounds) relative to the control simulation ($+0.41 \text{ W m}^{-2} \text{ K}^{-1}$) and excludes negative feedbacks (>99% confidence), in line with estimates based on multiple lines of evidence (Forster et al., 2021). Two of the significant parameters listed in Section 3.2 tend towards agreement with the control settings (`clubb_C2rt` and `micro_mg_autocon_nd_exp`), while `seasalt_emis_scale` differs from the control settings, tending towards higher values.

Parameters impacting cloud ice content tend towards reducing ice in the base state. `micro_mg_dcs` (controlling the size threshold for the autoconversion of cloud ice particles to snow) tends towards lower values than the control, which causes a higher precipitation efficiency in mixed phase clouds, shortening their lifetime, and increase sinks for cloud ice particles. Constrained parameter settings reduce the freezing activation of aerosols by scaling down vertical velocities in A/A module calculations (lower `microp_aero_wsubi_scale`).

`microp_aero_wsubi_min` has a slight tendency towards higher values, also reducing the freezing activation of aerosols. Constrained parameter settings for warm rain formation (`micro_mg_autocon_lwp_exp` and `micro_mg_accr_enhan_fact`, which enhances accretion rates) would reduce warm rain efficiency. These effects contribute to longer cloud lifetimes, which would reduce the control simulation’s too-dark subtropical cloud albedo bias (Figure 1a-b).

The sum effects of parameter tendencies controlling autoconversion and mixed phase processes are to trade warm rain formation efficiency for higher mixed phase precipitation efficiency. The impact of these constrained settings is reduced cloud ice content in the base state, weakening the negative feedback gained from the transition of cloud ice to liquid water with warming. This has been found to contribute to stronger positive SW cloud feedbacks among models (Bjordal et al., 2020).

Constrained settings for `clubb_C14` tend towards dissipating less turbulence than the control. Similarly, one CLUBB parameter that damps vertical wind variance and thus dissipates turbulence (`clubb_C1`) tends towards less damping than the control. These decreased turbulent dissipation settings increase cloud fraction and LWP (Figures S6 and S8, respectively). Other CLUBB parameters that impact LCC, `clubb_C6rtb` (and likewise `clubb_C6thlb`) and `clubb_gamma_coef`, tend towards lower settings that decrease in-cloud vertical moisture fluxes and variances in vertical distributions, respectively, relative to the control. These tendencies favors stratocumulus over cumulus growth in the subtropics and trade wind regions by retaining moisture in the boundary layer. In agreement with the control settings are the constrained distributions of the damping parameter for third-moment vertical velocity variances (`clubb_C8`), which tend towards high values, favoring stratocumulus growth.

The sum effect of constrained turbulence-related parameter tendencies would be to promote LCC in the base state by allowing turbulence and moisture to persist in the boundary layer, which would act to reduce too-weak subtropical R_{CRE} bias in the control simulation (Figure 1a). This also makes LCC more sensitive to dynamical conditions in ways that amplify LCC losses with warming; this is supported by analyzing the covariance between LCC reductions in warming scenario simulations and parameter settings in (Supplementary Figure S16), analogous to the maps in Figure 3.

Constrained settings for the deep convective cloud fraction parameter (`cldfrc_dp2`) tend to be lower than the control settings; this would lower deep convective cloud fraction and thus tropical albedo. The air mass entrainment rate parameter (`zmconv_dmpdz`) tends towards lower values in albedo symmetry-constrained distributions than the control. This would decrease LCC and albedo by drying the troposphere locally, but increase subtropical LCC due to the stronger subsidence necessitated by more intense tropical convection. Lower entrainment rates also make Hadley circulation strength more sensitive to warming and contribute to more positive low cloud feedbacks (Schiro et al., 2022). The associated SW cloud feedbacks would thus be more strongly positive as a result of weakening convection and subsidence leading to stronger LCC loss with warming (Supplementary Figure S16). Beyond SW cloud feedbacks, convective entrainment rates have implications for other feedbacks and climate sensitivity in other models (Mauritsen et al., 2012; Tomassini et al., 2015).

4 Discussion and Conclusions

We identified ten key parameters influencing simulated albedo asymmetry across a PPE of atmospheric simulations. Our findings highlight the cloud cover features that amplify simulated asymmetry through parametric uncertainties and indicate which processes are crucial. These parameters control precipitation efficiencies (impacting cloud lifetime), turbulence (impacting LCC), and sea salt aerosol emissions (impacting both

clear-sky and cloud albedo). The prominence of low cloud-related parameters underscores their role in hemispheric albedo symmetry. Given their significant contributions to planetary albedo (Wood, 2012) as well as total cloud feedbacks (Forster et al., 2021), this suggests that achieving realistic hemispheric albedo symmetry in models is relevant for predictions of future climate. LCC-determining processes that impact albedo asymmetry the most in the PPE are related to precipitation efficiency and turbulent dissipation. Precipitation-related parameters are most active in the extratropics and determine much of the variance in asymmetry across the PPE. Turbulence-related parameters primarily impact extratropical cloud amount. These effects are concentrated in the SH midlatitudes, highlighting their importance to the albedo symmetry.

We also constrain SW cloud feedbacks to the sector of the parameter space where albedo symmetry is reproduced and find them to be more strongly positive than those of the model’s control settings, and interpret the constrained parameter settings in order to explain these higher feedback strengths. Firstly, LCC is likely more sensitive to warming than in the control due to greater sensitivities to turbulence. This has the added effect of increasing LCC in the base state, which would reduce subtropical albedo biases seen in the control simulation. Secondly, warm rain formation may be overly efficient in the control simulation, which may be compensated for by underestimated mixed-phase precipitation formation. The effects of the constrained parameter settings on the base state are twofold: liquid clouds would be longer lived, and cloud ice content would be reduced due to greater cloud ice sinks. The tradeoff between higher mixed phase precipitation efficiencies and lower warm rain formation rates would have minimal impacts on midlatitude cloud albedo, but the reduced base state cloud ice content would yield weaker negative midlatitude cloud phase feedbacks. Lastly, base state tropical convective cloud amount would be reduced and deep convection would be stronger due to reduced entrainment. The latter would lead to tropospheric drying and reduced LCC in the tropics. These would reduce tropical biases seen in the control simulation, and the increased sensitivity of Hadley circulation would lead to more positive cloud feedbacks.

Our hypothesis that reproducing the hemispheric albedo symmetry in a model has implications for the strengths of SW cloud feedbacks follows from the reasoning that it would necessarily require bulk spatial features of global cloud cover to be reproduced. This would ideally arise from reduced compensating errors and more accurately represented cloud cover- and albedo-determining processes; that the constrained parameter settings tend towards reducing biases present in the PPE’s control simulation supports this being the case. We therefore propose that the observed hemispheric albedo symmetry may be a useful tuning guide for climate models by not only improving model cloud representation, but also constraining SW cloud radiative feedbacks. However, in order to better constrain SW cloud feedbacks, more constraints are necessary; promising candidates are LWP and f , as discussed around Figure 2. Our results illustrate the usefulness of the PPE in representing the spread of albedo symmetry in GCMs and leading us to processes relevant to establishing albedo symmetry.

5 Open Research

The CAM6 PPE output is public available at the Climate Data Gateway at NCAR (<https://doi.org/10.26024/bzne-yf09>). CMIP6 output is available through the Earth System Grid Federation (<https://esgf.llnl.gov/>). The code for reproducing the computations and figures in this study are hosted at <https://codeberg.org/aidenrobert>.

Author contributions

We follow the Contributor Roles Taxonomy (CRediT) guidelines. A.J. led the conceptualization, investigation, formal analysis, methodology, visualization, and writing (original draft preparation) of the work. M.R. led the supervision (equal) of the work, and

contributed to resource acquisition, conceptualization, formal analysis, investigation, and writing (review and editing). F.B. led the project administration, funding acquisition, and supervision (equal) of the work, and contributed to conceptualization, formal analysis, investigation, and writing (review and editing). D.M. contributed to the resource acquisition, data curation, investigation, formal analysis, and writing (review and editing). T.E. conducted the simulations to create the PPE, led the data curation and software for the work, and contributed to the writing (review and editing).

Competing interests

The authors declare no competing interests.

Acknowledgments

This research is part of a project funded by the Swedish Research Council (Grant 2018-04274). M.R. is supported by the National Science Foundation under Grant No. 2233673. D.M. is supported under NASA-PMMST Grant #80NSSC22K0599 and DOE-ASR Grant #DE-SC0022227. T.E. is supported under the NASA Grant #80NSSC17K0073. We would like to acknowledge the use of computational resources (doi:10.5065/D6RX99HX) at the NCAR-Wyoming Supercomputing Center provided by the National Science Foundation and the State of Wyoming, and supported by NCAR's Computational and Information Systems Laboratory including through the Wyoming-NCAR alliance large allocation WYOM0124. For their comments, guidance, and advice on this study, we are thankful to Ci Song, Andrew Gettelman, Maura Dewey, George Datseris, and Xiang-Yu Li.

References

- Bender, F. A.-M. (2008). A note on the effect of GCM tuning on climate sensitivity. *Environmental Research Letters*, 3(1), 014001. doi: 10.1088/1748-9326/3/1/014001
- Bender, F. A.-M., Engström, A., Wood, R., & Charlson, R. J. (2017). Evaluation of Hemispheric Asymmetries in Marine Cloud Radiative Properties. *Journal of Climate*, 30(11), 4131 - 4147. doi: 10.1175/JCLI-D-16-0263.1
- Bjordal, J., Storelvmo, T., Alterskjær, K., & Carlsen, T. (2020, Nov 01). Equilibrium climate sensitivity above 5 °C plausible due to state-dependent cloud feedback. *Nature Geoscience*, 13(11), 718-721. doi: 10.1038/s41561-020-00649-1
- Blanco, J. E., Caballero, R., Datseris, G., Stevens, B., Bony, S., Hadas, O., & Kaspi, Y. (2023). A Cloud-Controlling Factor Perspective on the Hemispheric Asymmetry of Extratropical Cloud Albedo. *Journal of Climate*, 36(6), 1793 - 1804. doi: <https://doi.org/10.1175/JCLI-D-22-0410.1>
- Bodas-Salcedo, A., Hill, P. G., Furtado, K., Williams, K. D., Field, P. R., Manners, J. C., ... Kato, S. (2016). Large Contribution of Supercooled Liquid Clouds to the Solar Radiation Budget of the Southern Ocean. *Journal of Climate*, 29(11), 4213 - 4228. doi: <https://doi.org/10.1175/JCLI-D-15-0564.1>
- Bodas-Salcedo, A., Williams, K. D., Ringer, M. A., Beau, I., Cole, J. N. S., Dufresne, J.-L., ... Yokohata, T. (2014). Origins of the Solar Radiation Biases over the Southern Ocean in CFMIP2 Models. *Journal of Climate*, 27(1), 41 - 56. doi: <https://doi.org/10.1175/JCLI-D-13-00169.1>
- Bogenschütz, P. A., Gettelman, A., Morrison, H., Larson, V. E., Craig, C., & Schanen, D. P. (2013). Higher-Order Turbulence Closure and Its Impact on Climate Simulations in the Community Atmosphere Model. *Journal of Climate*, 26(23), 9655 - 9676. doi: <https://doi.org/10.1175/JCLI-D-13-00075.1>
- Carlsaw, K. S., Lee, L. A., Reddington, C. L., Pringle, K. J., Rap, A., Forster, P. M., ... Pierce, J. R. (2013, Nov 01). Large contribution of natural

- aerosols to uncertainty in indirect forcing. *Nature*, 503(7474), 67-71. doi: 10.1038/nature12674
- Chemke, R., Ming, Y., & Yuval, J. (2022, Jun 01). The intensification of winter mid-latitude storm tracks in the Southern Hemisphere. *Nature Climate Change*, 12(6), 553-557. doi: 10.1038/s41558-022-01368-8
- Cover, T., & Thomas, J. (2005). Entropy, Relative Entropy, and Mutual Information. In *Elements of Information Theory* (p. 13-55). John Wiley & Sons, Ltd. doi: <https://doi.org/10.1002/047174882X.ch2>
- Crueger, T., Schmidt, H., & Stevens, B. (2023). Hemispheric Albedo Asymmetries across Three Phases of CMIP. *Journal of Climate*, 36(15), 5267 - 5280. doi: <https://doi.org/10.1175/JCLI-D-22-0923.1>
- Danabasoglu, G., Lamarque, J.-F., Bacmeister, J., Bailey, D. A., DuVivier, A. K., Edwards, J., ... Strand, W. G. (2020). The Community Earth System Model Version 2 (CESM2). *Journal of Advances in Modeling Earth Systems*, 12(2), e2019MS001916. doi: <https://doi.org/10.1029/2019MS001916>
- Datseris, G., & Stevens, B. (2021). Earth's Albedo and Its Symmetry. *AGU Advances*, 2(3), e2021AV000440. doi: <https://doi.org/10.1029/2021AV000440>
- de Leeuw, G., Andreas, E. L., Anguelova, M. D., Fairall, C. W., Lewis, E. R., O'Dowd, C., ... Schwartz, S. E. (2011). Production flux of sea spray aerosol. *Reviews of Geophysics*, 49(2). doi: <https://doi.org/10.1029/2010RG000349>
- Diamond, M. S., Gristey, J. J., Kay, J. E., & Feingold, G. (2022, Sep 12). Anthropogenic aerosol and cryosphere changes drive earth's strong but transient clear-sky hemispheric albedo asymmetry. *Communications Earth & Environment*, 3(1), 206. doi: 10.1038/s43247-022-00546-y
- Dommenget, D. (2016, Jan 01). A simple model perturbed physics study of the simulated climate sensitivity uncertainty and its relation to control climate biases. *Climate Dynamics*, 46(1), 427-447. doi: 10.1007/s00382-015-2591-4
- Eidhammer, T., Andrew Gettelman, A., Thayer-Calder, K., Watson-Parris, D., Elsaesser, G., Morrison, H., ... McCoy, D. (2023). An Extensible Perturbed Parameter Ensemble (PPE) for the Community Atmosphere Model Version 6. *Submitted to Geoscientific Model Development*.
- Eyring, V., Bony, S., Meehl, G. A., Senior, C. A., Stevens, B., Stouffer, R. J., & Taylor, K. E. (2016). Overview of the Coupled Model Intercomparison Project Phase 6 (CMIP6) experimental design and organization. *Geoscientific Model Development*, 9(5), 1937-1958. doi: 10.5194/gmd-9-1937-2016
- Fan, J., Wang, Y., Rosenfeld, D., & Liu, X. (2016). Review of Aerosol-Cloud Interactions: Mechanisms, Significance, and Challenges. *Journal of the Atmospheric Sciences*, 73(11), 4221 - 4252. doi: <https://doi.org/10.1175/JAS-D-16-0037.1>
- Fiddes, S. L., Protat, A., Mallet, M. D., Alexander, S. P., & Woodhouse, M. T. (2022). Southern Ocean cloud and shortwave radiation biases in a nudged climate model simulation: does the model ever get it right? *Atmospheric Chemistry and Physics*, 22(22), 14603-14630. doi: 10.5194/acp-22-14603-2022
- Forster, P., Storelvmo, T., Armour, K., Collins, W., Dufresne, J. L., Frame, D., ... Zhang, H. (2021). The Earth's Energy Budget, Climate Feedbacks, and Climate Sensitivity [Book Section]. In V. Masson-Delmotte et al. (Eds.), *Climate Change 2021: The Physical Science Basis. Contribution of Working Group I to the Sixth Assessment Report of the Intergovernmental Panel on Climate Change* (p. 923-1054). Cambridge, United Kingdom and New York, NY, USA: Cambridge University Press. doi: 10.1017/9781009157896.009
- Gettelman, A., & Morrison, H. (2015). Advanced Two-Moment Bulk Microphysics for Global Models. Part I: Off-Line Tests and Comparison with Other Schemes. *Journal of Climate*, 28(3), 1268 - 1287. doi: <https://doi.org/10.1175/JCLI-D-14-00102.1>
- Gettelman, A., Morrison, H., Santos, S., Bogenschutz, P., & Caldwell, P. M. (2015). Advanced Two-Moment Bulk Microphysics for Global Models. Part II: Global

- Model Solutions and Aerosol–Cloud Interactions. *Journal of Climate*, 28(3), 1288 - 1307. doi: <https://doi.org/10.1175/JCLI-D-14-00103.1>
- Golaz, J.-C., Caldwell, P. M., Van Roekel, L. P., Petersen, M. R., Tang, Q., Wolfe, J. D., ... Zhu, Q. (2019). The DOE E3SM Coupled Model Version 1: Overview and Evaluation at Standard Resolution. *Journal of Advances in Modeling Earth Systems*, 11(7), 2089-2129. doi: <https://doi.org/10.1029/2018MS001603>
- Golaz, J.-C., Larson, V. E., & Cotton, W. R. (2002). A PDF-Based Model for Boundary Layer Clouds. Part I: Method and Model Description. *Journal of the Atmospheric Sciences*, 59(24), 3540 - 3551. doi: [https://doi.org/10.1175/1520-0469\(2002\)059<3540:APBMFB>2.0.CO;2](https://doi.org/10.1175/1520-0469(2002)059<3540:APBMFB>2.0.CO;2)
- Golaz, J.-C., Van Roekel, L. P., Zheng, X., Roberts, A. F., Wolfe, J. D., Lin, W., ... Bader, D. C. (2022). The DOE E3SM Model Version 2: Overview of the Physical Model and Initial Model Evaluation. *Journal of Advances in Modeling Earth Systems*, 14(12), e2022MS003156. doi: <https://doi.org/10.1029/2022MS003156>
- Guo, Z., Wang, M., Qian, Y., Larson, V. E., Ghan, S., Ovchinnikov, M., ... Zhou, T. (2015). Parametric behaviors of CLUBB in simulations of low clouds in the Community Atmosphere Model (CAM). *Journal of Advances in Modeling Earth Systems*, 7(3), 1005-1025. doi: <https://doi.org/10.1002/2014MS000405>
- Hadas, O., Datseris, G., Blanco, J., Bony, S., Caballero, R., Stevens, B., & Kaspi, Y. (2023). The role of baroclinic activity in controlling Earth's albedo in the present and future climates. *Proceedings of the National Academy of Sciences*, 120(5), e2208778120. doi: [10.1073/pnas.2208778120](https://doi.org/10.1073/pnas.2208778120)
- Hartery, S., Toohey, D., Revell, L., Sellegri, K., Kuma, P., Harvey, M., & McDonald, A. J. (2020). Constraining the Surface Flux of Sea Spray Particles From the Southern Ocean. *Journal of Geophysical Research: Atmospheres*, 125(4), e2019JD032026. doi: <https://doi.org/10.1029/2019JD032026>
- Hourdin, F., Mauritsen, T., Gettelman, A., Golaz, J.-C., Balaji, V., Duan, Q., ... Williamson, D. (2017). The Art and Science of Climate Model Tuning. *Bulletin of the American Meteorological Society*, 98(3), 589 - 602. doi: <https://doi.org/10.1175/BAMS-D-15-00135.1>
- Hwang, Y.-T., & Frierson, D. M. W. (2013). Link between the double-Intertropical Convergence Zone problem and cloud biases over the Southern Ocean. *Proceedings of the National Academy of Sciences*, 110(13), 4935-4940. doi: [10.1073/pnas.1213302110](https://doi.org/10.1073/pnas.1213302110)
- Hyder, P., Edwards, J. M., Allan, R. P., Hewitt, H. T., Bracegirdle, T. J., Gregory, J. M., ... Belcher, S. E. (2018, Sep 11). Critical Southern Ocean climate model biases traced to atmospheric model cloud errors. *Nature Communications*, 9(1), 3625. doi: [10.1038/s41467-018-05634-2](https://doi.org/10.1038/s41467-018-05634-2)
- Jönsson, A. R., & Bender, F. A.-M. (2023). The implications of maintaining Earth's hemispheric albedo symmetry for shortwave radiative feedbacks. *Earth System Dynamics*, 14(2), 345-365. doi: [10.5194/esd-14-345-2023](https://doi.org/10.5194/esd-14-345-2023)
- Jönsson, A., & Bender, F. A.-M. (2022). Persistence and Variability of Earth's Interhemispheric Albedo Symmetry in 19 Years of CERES EBAF Observations. *Journal of Climate*, 35(1), 249 - 268. doi: <https://doi.org/10.1175/JCLI-D-20-0970.1>
- Kajtar, J. B., Santoso, A., Collins, M., Taschetto, A. S., England, M. H., & Frankcombe, L. M. (2021). CMIP5 Intermodel Relationships in the Baseline Southern Ocean Climate System and With Future Projections. *Earth's Future*, 9(6), e2020EF001873. doi: <https://doi.org/10.1029/2020EF001873>
- Kay, J. E., Wall, C., Yettella, V., Medeiros, B., Hannay, C., Caldwell, P., & Bitz, C. (2016). Global Climate Impacts of Fixing the Southern Ocean Shortwave Radiation Bias in the Community Earth System Model (CESM). *Journal of Climate*, 29(12), 4617 - 4636. doi: <https://doi.org/10.1175/JCLI-D-15-0358.1>

- Khairoutdinov, M., & Kogan, Y. (2000). A New Cloud Physics Parameterization in a Large-Eddy Simulation Model of Marine Stratocumulus. *Monthly Weather Review*, 128(1), 229 - 243. doi: [https://doi.org/10.1175/1520-0493\(2000\)128<0229:ANCPPI>2.0.CO;2](https://doi.org/10.1175/1520-0493(2000)128<0229:ANCPPI>2.0.CO;2)
- Kim, H., Kang, S. M., Kay, J. E., & Xie, S.-P. (2022). Subtropical clouds key to Southern Ocean teleconnections to the tropical Pacific. *Proceedings of the National Academy of Sciences*, 119(34), e2200514119. doi: 10.1073/pnas.2200514119
- Mauritsen, T., Stevens, B., Roeckner, E., Crueger, T., Esch, M., Giorgetta, M., ... Tomassini, L. (2012). Tuning the climate of a global model. *Journal of Advances in Modeling Earth Systems*, 4(3). doi: <https://doi.org/10.1029/2012MS000154>
- McCoy, D. T., Burrows, S. M., Wood, R., Grosvenor, D. P., Elliott, S. M., Ma, P.-L., ... Hartmann, D. L. (2015). Natural aerosols explain seasonal and spatial patterns of Southern Ocean cloud albedo. *Science Advances*, 1(6), e1500157. doi: 10.1126/sciadv.1500157
- Mechoso, C. R., Losada, T., Koseki, S., Mohino-Harris, E., Keenlyside, N., Castaño-Tierno, A., ... Toniazzo, T. (2016). Can reducing the incoming energy flux over the Southern Ocean in a CGCM improve its simulation of tropical climate? *Geophysical Research Letters*, 43(20), 11,057-11,063. doi: <https://doi.org/10.1002/2016GL071150>
- Nam, C., Bony, S., Dufresne, J.-L., & Chepfer, H. (2012). The ‘too few, too bright’ tropical low-cloud problem in CMIP5 models. *Geophysical Research Letters*, 39(21). doi: <https://doi.org/10.1029/2012GL053421>
- NASA/LARC/SD/ASDC. (2019, 6 12). *CERES Energy Balanced and Filled (EBAF) TOA and Surface Monthly means data in netCDF Edition 4.1*. NASA Langley Atmospheric Science Data Center DAAC. doi: 10.5067/TERRA-AQUA/CERES/EBAF_L3B.004.1
- Priestley, M. D. K., Ackerley, D., Catto, J. L., & Hodges, K. I. (2023). Drivers of Biases in the CMIP6 Extratropical Storm Tracks. Part II: Southern Hemisphere. *Journal of Climate*, 36(5), 1469 - 1486. doi: <https://doi.org/10.1175/JCLI-D-20-0977.1>
- Rugenstein, M., Dhame, S., Olonscheck, D., Wills, R. J., Watanabe, M., & Seager, R. (2023). Connecting the SST Pattern Problem and the Hot Model Problem. *Geophysical Research Letters*, 50(22), e2023GL105488. (e2023GL105488) doi: <https://doi.org/10.1029/2023GL105488>
- Rugenstein, M., & Hakuba, M. (2023). Connecting hemispheric asymmetries of planetary albedo and surface temperature. *Geophysical Research Letters*, 50(6), e2022GL101802. doi: <https://doi.org/10.1029/2022GL101802>
- Schiro, K. A., Su, H., Ahmed, F., Dai, N., Singer, C. E., Gentine, P., ... David Neelin, J. (2022, Nov 19). Model spread in tropical low cloud feedback tied to overturning circulation response to warming. *Nature Communications*, 13(1), 7119. doi: 10.1038/s41467-022-34787-4
- Shaw, T. A., Miyawaki, O., & Donohoe, A. (2022). Stormier Southern Hemisphere induced by topography and ocean circulation. *Proceedings of the National Academy of Sciences*, 119(50), e2123512119. doi: 10.1073/pnas.2123512119
- Stephens, G. L., O’Brien, D., Webster, P. J., Pilewski, P., Kato, S., & Li, J.-l. (2015). The albedo of earth. *Reviews of Geophysics*, 53(1), 141-163. doi: <https://doi.org/10.1002/2014RG000449>
- Stevens, B., & Schwartz, S. E. (2012, Jul 01). Observing and Modeling Earth’s Energy Flows. *Surveys in Geophysics*, 33(3), 779-816. doi: 10.1007/s10712-012-9184-0
- Szopa, S., Naik, V., Adhikary, B., Artaxo, P., Bernsten, T., Collins, W., ... Zanis, P. (2021). Short-Lived Climate Forcers [Book Section]. In V. Masson-Delmotte et al. (Eds.), *Climate change 2021: The physical science basis. contribution of*

- working group i to the sixth assessment report of the intergovernmental panel on climate change (p. 817–922). Cambridge, United Kingdom and New York, NY, USA: Cambridge University Press. doi: 10.1017/9781009157896.008
- Tomassini, L., Voigt, A., & Stevens, B. (2015). On the connection between tropical circulation, convective mixing, and climate sensitivity. *Quarterly Journal of the Royal Meteorological Society*, 141(689), 1404–1416. doi: <https://doi.org/10.1002/qj.2450>
- Tsigaridis, K., Koch, D., & Menon, S. (2013). Uncertainties and importance of sea spray composition on aerosol direct and indirect effects. *Journal of Geophysical Research: Atmospheres*, 118(1), 220–235. doi: <https://doi.org/10.1029/2012JD018165>
- Vergara-Temprado, J., Miltenberger, A. K., Furtado, K., Grosvenor, D. P., Shipway, B. J., Hill, A. A., ... Carslaw, K. S. (2018). Strong control of Southern Ocean cloud reflectivity by ice-nucleating particles. *Proceedings of the National Academy of Sciences*, 115(11), 2687–2692. doi: 10.1073/pnas.1721627115
- Voigt, A., Stevens, B., Bader, J., & Mauritsen, T. (2013). The observed hemispheric symmetry in reflected shortwave irradiance. *Journal of Climate*, 26(2), 468–477.
- Voigt, A., Stevens, B., Bader, J., & Mauritsen, T. (2014). Compensation of Hemispheric Albedo Asymmetries by Shifts of the ITCZ and Tropical Clouds. *Journal of Climate*, 27(3), 1029 - 1045. doi: 10.1175/JCLI-D-13-00205.1
- Vonder Haar, T. H., & Suomi, V. E. (1971). Measurements of the Earth’s Radiation Budget from Satellites During a Five-Year Period. Part I: Extended Time and Space Means. *Journal of Atmospheric Sciences*, 28(3), 305–314. doi: 10.1175/1520-0469(1971)028<0305:MOTERB>2.0.CO;2
- Watson-Parris, D., Williams, A., Deaconu, L., & Stier, P. (2021). Model calibration using ESEm v1.1.0 – an open, scalable Earth system emulator. *Geoscientific Model Development*, 14(12), 7659–7672. doi: 10.5194/gmd-14-7659-2021
- Wood, R. (2012). Stratocumulus Clouds. *Monthly Weather Review*, 140(8), 2373 - 2423. doi: <https://doi.org/10.1175/MWR-D-11-00121.1>
- Zelinka, M. D., Klein, S. A., Qin, Y., & Myers, T. A. (2022). Evaluating climate models’ cloud feedbacks against expert judgment. *Journal of Geophysical Research: Atmospheres*, 127(2), e2021JD035198. doi: <https://doi.org/10.1029/2021JD035198>
- Zhang, G., & McFarlane, N. A. (1995). Sensitivity of climate simulations to the parameterization of cumulus convection in the Canadian climate centre general circulation model. *Atmosphere-Ocean*, 33(3), 407–446. doi: 10.1080/07055900.1995.9649539
- Zhao, L., Wang, Y., Zhao, C., Dong, X., & Yung, Y. L. (2022, Dec 01). Compensating Errors in Cloud Radiative and Physical Properties over the Southern Ocean in the CMIP6 Climate Models. *Advances in Atmospheric Sciences*, 39(12), 2156–2171. doi: 10.1007/s00376-022-2036-z